

Analyst

Accepted Manuscript



This is an *Accepted Manuscript*, which has been through the Royal Society of Chemistry peer review process and has been accepted for publication.

Accepted Manuscripts are published online shortly after acceptance, before technical editing, formatting and proof reading. Using this free service, authors can make their results available to the community, in citable form, before we publish the edited article. We will replace this *Accepted Manuscript* with the edited and formatted *Advance Article* as soon as it is available.

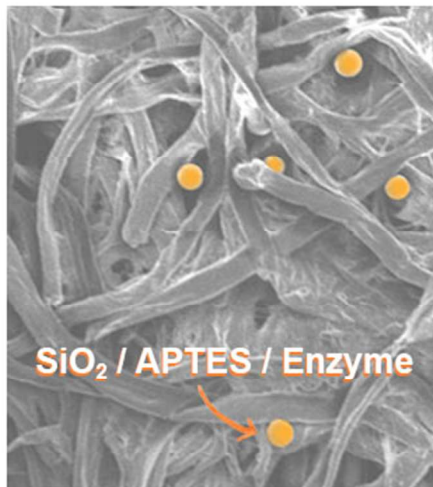
You can find more information about *Accepted Manuscripts* in the [Information for Authors](#).

Please note that technical editing may introduce minor changes to the text and/or graphics, which may alter content. The journal's standard [Terms & Conditions](#) and the [Ethical guidelines](#) still apply. In no event shall the Royal Society of Chemistry be held responsible for any errors or omissions in this *Accepted Manuscript* or any consequences arising from the use of any information it contains.

1
2
3
4
5
6
7
8
9
10
11
12
13
14
15
16
17
18
19
20
21
22
23
24
25
26
27
28
29
30
31
32
33
34
35
36
37
38
39
40
41
42
43
44
45
46
47
48
49
50
51
52
53
54
55
56
57
58
59
60

Table of Contents Entry

Modification of μ PADs with SiO_2 NP provide enhanced color intensity and minimal color gradient



1
2
3
4
5
6
7
8
9
10
11
12
13
14
15
16
17
18
19
20
21
22
23
24
25
26
27
28
29
30
31
32
33
34
35
36
37
38
39
40
41
42
43
44
45
46
47
48
49
50
51
52
53
54
55
56

Modification of Microfluidic Paper-Based Devices with Silica Nanoparticles

Elizabeth Evans¹, Ellen Flávia Moreira Gabriel^{1,2}, Tomás E. Benavidez¹, Wendell Karlos Tomazelli Coltro², and Carlos D. Garcia^{1*}

¹Department of Chemistry, The University of Texas at San Antonio, San Antonio, TX, 78249, USA.

²Instituto de Química, Universidade Federal de Goiás, Goiânia, GO, 74001970, Brazil.

57
58
59
60

* **Corresponding author:** Carlos D. Garcia, One UTSA Circle, San Antonio, TX, 78249, Phone: (210) 458-5774, Fax: (210) 458-5774, E-mail: carlos.garcia@utsa.edu

Abstract

This paper describes a silica nanoparticle-modified microfluidic paper-based analytical device (μ PAD) with improved color intensity and uniformity for three different enzymatic reactions with clinical relevance (lactate, glucose, and glutamate). The μ PADs were produced on Whatman grade 1 filter paper and using a CO₂ laser engraver. Silica nanoparticles modified with 3-aminopropyltriethoxysilane (APTES) were then added to the paper devices to facilitate the adsorption of selected enzymes and prevent the washing away effect that creates color gradients in the colorimetric measurements. Here we show three different enzymatic assays for compounds. According to the results herein described, the addition of silica nanoparticles yielded to significant improvements in color intensity and uniformity. The resulting μ PADs allowed for the detection of the three analytes in clinically-relevant concentration ranges with limits of detection (LOD) of 0.63 mM, 0.50 mM, and 0.25 mM for lactate, glucose, and glutamate, respectively. An example of an analytical application has been demonstrated for the semi-quantitative detection of all three analytes in artificial urine. The results demonstrate the potential of silica nanoparticles to avoid the washing away effect and improve the color uniformity and intensity in colorimetric bioassays performed on μ PADs.

1
2
3 **Keywords:** Immobilization process, nanomaterials, CO₂-laser, colorimetric assays, μPADs
4
5
6
7
8
9
10
11
12
13
14
15
16
17
18
19
20
21
22
23
24
25
26
27
28
29
30
31
32
33
34
35
36
37
38
39
40
41
42
43
44
45
46
47
48
49
50
51
52
53
54
55
56
57
58
59
60

1. INTRODUCTION

In the last decade, the interest to develop paper-based analytical platforms has grown exponentially. Their low-cost, availability of different fabrication techniques, safe disposal, low consumption of reagents and sample, high potential for remote use, and capability to provide semi-quantitative results for a series of analytes are some of the top reasons behind the success of microfluidic paper-based analytical devices (μ PADs).¹⁻⁵ Furthermore, since their initial development, μ PADs have been employed for a variety of applications including immunoassays,⁶ environmental monitoring,^{7, 8} bioterrorism,⁹ and urinalysis.^{3, 10} While there are many detection methods for μ PADs, such as electrochemical,¹¹ transmittance,¹² electrochemiluminescence,¹³ chemiluminescence,^{6, 14} and fluorescence,^{9, 15} colorimetric detection¹⁶⁻¹⁹ has been the most widely adopted technique for μ PADs. The success of this detection method can be attributed to the simplicity of the final response, which can be converted to a semi-quantitative numerical value using a calibration curve obtained with an image from a cellphone camera or portable scanner. Most often, these assays are based on the selective oxidation of the analyte followed by a peroxidase-based reaction²⁰ that catalyzes the oxidation of a chromogenic agent^{21, 22} that yields to a color change.²³ Although there are several drawbacks associated with this technology, the most remarkable one is the heterogeneity of the color distribution in the detection zones. This issue, which can be attributed to the mobility of enzymes and reagents towards the edge of the detection zone when the sample wicks up the hydrophilic channels, can result in increased variability and poor judgment of the final color by the user.^{1, 24} Several strategies can be adopted to overcome this problem, including controlling the volume of reactants and the sample's wicking velocity.²⁵ Among those directed to the immobilization of the enzymes via chemical modification to the cellulose²⁶⁻²⁸ it is worth mentioning the addition of succinic anhydride,²⁹ sodium periodate,³⁰ or 3-aminopropyltrimethoxysilane (APTES).³¹ These modifications result in the formation of carbonyl, aldehyde, or amino groups than can be used to permanently immobilize enzymes using covalent bonds and well-known conditions. μ PADs can also be modified using ceria nanoparticles,²² gold nanoparticles,³² silver nanoparticles,^{33, 34} and carbon nanotubes^{35, 36} to aid with the detection step. Although each of these strategies presents their own advantages, they are not widely applicable and require the implementation of specific processes. Aiming to address these shortcomings, the hypothesis of this project was that silica nanoparticles, trapped within

1
2
3 the structure of the cellulose, could provide a simple and efficient way to immobilize the components of
4 the analysis and therefore improve the overall performance of colorimetric detection on μ PADs. Due to
5 their clinical relevance^{17, 37, 38} the experiments herein described were focused on the analysis of lactate,
6 glucose, and glutamate in artificial urine; providing a non-invasive and highly abundant sample to assess
7 the effectiveness of the proposed strategy.
8
9
10
11
12

13 14 15 **2. EXPERIMENTAL SECTION**

16
17 **2.1 Material and Reagents.** Glucose oxidase (from *Aspergillus niger*, 17300 U·g⁻¹) (GOx), peroxidase
18 type II (from horseradish 199 pupurogallin, U·mg⁻¹) (HRP), lactate oxidase (from *Pediococcus* sp. 20
21 U·mg⁻¹) (LOx), L-glutamate oxidase (from *Streptomyces* sp., 5 U·mg⁻¹) (LGOx), D-(+)-glucose, sodium-L-
22 lactate, sodium 3,5-dichloro-2-hydroxy-benzenesulfonic acid (DHBS), 3-aminopropyltriethoxysilane (99%)
23 (APTES), silicon dioxide nanopowder (15 nm), ethanol (99.5%), L-glutamic acid (Glu), 3,3',5,5'-
24 tetramethylbenzidine \geq 98% (TMB), citric acid, sodium bicarbonate, urea, sodium sulfate, and ammonium
25 chloride were purchased from Sigma-Aldrich (St. Louis, MO). 4-aminoantipyrine (AAP) was obtained from
26 Alfa Aesar (Ward Hill, MA). Calcium chloride and potassium iodide (KI) were purchased from E.M.
27 Science (Gibbstown, NJ). Sodium phosphate monobasic anhydrous and sodium phosphate dibasic
28 anhydrous were received from Fisher Scientific (Waltham, MA). D-(+)-trehalose anhydrous was obtained
29 from TCI American (Portland, OR). Sodium chloride and magnesium sulfate were purchased from
30 Mallinckrodt Baker (now Avantor Performance Materials; Center Valley, PA). Following a recent
31 publication from our group,²⁵ experiments were carried out on filter paper #1, obtained from Whatman
32 (Maidson Kent, UK). All chemicals were used as received and made in ultrapure water (18 M Ω ·cm⁻¹,
33 Barnstead Nanopure; Dubuque, IA) without further purification. For the analysis, a standard solution
34 containing the highest concentrations of each analyte (25 mmol·L⁻¹ lactate, 20 mmol·L⁻¹ glucose, and 10
35 mmol·L⁻¹ glutamate) was prepared in 100 mmol·L⁻¹ PBS (pH=6.0) and diluted at different ratios to cover
36 the concentration ranges utilized in the calibration curves.
37
38
39
40
41
42
43
44
45
46
47
48
49
50
51

52 The ellipsometry experiments were performed using standard <111> silicon wafers (Si/SiO₂, Sumco
53 Corporation; Phoenix, AZ) that were scored using a computer-controlled engraver (Gravograph IS400,
54 Gravotech; Duluth, GA). The substrates were then manually cut (1 cm in width and 4 cm in length),
55
56
57
58
59
60

1
2
3 cleaned in piranha solution (30% H₂O₂ : 70% sulfuric acid) at 90 °C for 30 min, thoroughly rinsed it with DI
4
5 water, and dried in a convective oven.
6
7

8
9 **2.2 Instrumentation.** Numerous techniques have been employed for the fabrication of μ PADs, including
10 photolithography, plotting, screen printing, inkjet etching, plasma etching, inkjet printing, flexographic
11 printing, PDMS printing, printed circuit technology, laser cutting, and wax printing.^{1, 2, 39, 40} Among the
12 diverse fabrication procedures, laser cutting from a predesigned pattern is a one-step straightforward
13 method for fabrication of μ PADs.¹⁶ For that reason, a commercial CO₂ laser engraver (Mini 24, 30W,
14 Epilog Laser Systems; Golden, CO) was used to cut the paper and produce the μ PADs. Details about the
15 system and its capabilities can be found elsewhere.⁴¹ This system was connected to an air filter (model
16 AD350, BOFA; Staunton, IL), equipped with a HEPA / activated aluminum / potassium permanganate and
17 an activated carbon panel to remove fumes from the engraver. To minimize the risk of ignition of the
18 paper during the cutting process, a stream of N₂ was impinged on the engraving point. The layout for the
19 μ PAD was designed using CorelDraw X6 and cut using 600-dpi resolution, 30% power, and 30% speed.
20 This process resulted in the ablation of the edge of the microfluidic design and the creation of a
21 hydrophobic boundary.¹⁶ To gain insight about the density and distribution of the SiO₂ nanoparticles on
22 the paper, scanning electron microscopy (SEM, JEOL/EO, JSM-6510; Peabody, MA) was used.
23
24
25
26
27
28
29
30
31
32
33
34
35
36
37
38

39 **2.3 Enzymatic Solutions and Colorimetric Detection.** All assays were prepared using solutions
40 containing either a mixture of the enzymes or the chromogenic agent. For the glucose assay, a 1:5
41 mixture of HRP (339 U·mL⁻¹, in 100 mmol·L⁻¹ PBS pH=6.0) and GOx (645 U·mL⁻¹, in 100 mmol·L⁻¹ PBS
42 pH=6.0) was prepared. The chromogenic reagent was prepared using KI and trehalose, dissolved in 100
43 mmol·L⁻¹ PBS (pH=6.0) to a final concentration of 0.6 and 0.3 mol·L⁻¹, respectively. For the lactate
44 detection, a 1:1 mixture of LOx (100 U·mL⁻¹, in 100 mmol·L⁻¹ PBS pH=6.0) and HRP (339 U·mL⁻¹, in 100
45 mmol·L⁻¹ PBS pH=6.0) was prepared. In this case, 4-AAP and DHBS (6.6 mmol·L⁻¹) were dissolved in
46 100 mmol·L⁻¹ PBS (pH=6.0) and kept in the fridge covered with aluminum foil to refrain from light. For the
47 glutamate assay, a 1:1 mixture of LGOx (4.16 U·mL⁻¹, in 100 mmol·L⁻¹ PBS pH=7.4) and HRP (339 U·mL⁻¹
48
49
50
51
52
53
54
55
56
57
58
59
60

1
2
3
4
5
6
7
8
9
10
11
12
13
14
15
16
17
18
19
20
21
22
23
24
25
26
27
28
29
30
31
32
33
34
35
36
37
38
39
40
41
42
43
44
45
46
47
48
49
50
51
52
53
54
55
56
57
58
59
60

¹, in 100 mmol·L⁻¹ PBS pH=6) was prepared. TMB (15 mmol·L⁻¹, dissolved in EtOH and kept in the fridge covered in aluminum foil to refrain from light)⁴² was selected as the chromogenic agent.

The μ PADs were modified with silica nanoparticles (*vide infra*) and then thoroughly rinsed with PBS (pH = 6.0) to remove the excess particles from the surface of the paper. Afterwards, 1 μ L of the solution containing the selected enzymes was spotted on the detection zone and dried at room temperature for 15 min. Next, 1 μ L of the solution containing the selected chromogenic agent was spotted on the detection zone and dried at room temperature for another 15 min. Finally, solutions containing the analytes (10 μ L) were introduced to the μ PADs at the bottom extremity of the center channel and allowed to reach the detection zones by capillarity. After 30 min, an image of the device was acquired using a flatbed scanner (Canon, CanonScan Lide700F) and then analyzed using Adobe Photoshop CS6.

2.4 Artificial Urine Sample. In agreement with previous reports,^{11, 16, 43} the artificial urine was prepared at pH = 6.0 and comprised of 2 mM citric acid, 25 mM sodium bicarbonate, 170 mM urea, 2.5 mM calcium chloride, 90 mM sodium chloride, 2 mM magnesium sulfate, 10 mM sodium sulfate, 7 mM sodium phosphate monobasic anhydrous, 7 mM sodium phosphate dibasic anhydrous, and 25 mM ammonium chloride. This solution was stored in the refrigerator (4 °C) until use.

2.5 Spectroscopic Ellipsometry. Ellipsometric experiments, used to investigate the enzyme adsorption process to a SiO₂ substrate, were performed using a variable angle spectroscopic ellipsometer (WVASE, J.A. Woollam Co.; Lincoln, NE) following a procedure described elsewhere.⁴⁴⁻⁴⁶ The collected data (amplitude ratio (Ψ) and phase difference (Δ) as function of wavelength or time) was modeled using the WVASE software package (J.A. Woollam Co.; Lincoln, NE) and the mean square error (MSE, calculated by a built-in function in WVASE) was used to quantify the difference between the experimental and model-generated data. In agreement with previous reports, MSE < 15 were considered acceptable.^{45, 47} The ellipsometric measurements were interpreted using an optical model that considered the dielectric properties of Si (bulk, d = 1 mm) and SiO₂ (d = 2.1 \pm 0.5 nm). A standard Cauchy function was added to describe the optical properties of the APTES layer (d = 0.89 \pm 0.06 nm).⁴⁸ Finally, and when pertinent,

1
2
3 optical properties of the enzyme adsorbed on the substrates were also described with an additional
4 Cauchy function. Dynamic adsorption experiments, performed to determine the adsorption time, were
5 carried out in a modified electrochemical cell (J.A. Woollam Co.; Lincoln, NE) mounted directly on the
6 vertical base of the ellipsometer, with an incident angle of 70°. First, a spectroscopic scan of either the
7 silica wafer (Si/SiO₂) or the silica wafer modified with APTES (Si/SiO₂/APTES) was measured (from 300
8 to 800 nm, with 10 nm step) by placing the substrate in the ellipsometry cell using buffer solution (100
9 mmol·L⁻¹ PBS, pH=6.0) as the aqueous medium. Next, the adsorption experiment was started recording a
10 baseline while buffer solution was pumped with a peristaltic pump (Gilson Minipuls 3; Middleton, WI)
11 inside the cell at a rate of 1 mL·min⁻¹. After 20 min of baseline, the enzyme solution was injected to allow
12 the absorption of a monolayer of GOx on the substrate surface. When a plateau in the signal was noticed,
13 the buffer solution was pumped again into the cell for 20 minutes in order to evaluate the stability of GOx
14 layer formed on the substrate. Lastly, a spectroscopic scan was performed to obtain the thickness of the
15 enzyme layer; which allows calculating the change in thickness and adsorbed amount of GOx during the
16 dynamic adsorption experiment.
17
18
19
20
21
22
23
24
25
26
27
28
29
30
31
32

33 3. RESULTS AND DISCUSSION

34 Based on the current literature, it is clear that μ PADS represent one the most powerful tools in the field of
35 modern chemical analysis. However, the poor uniformity and homogeneity associated with colorimetric
36 measurements represent some the most important shortcomings of this technology. Aiming to solve this
37 problem, SiO₂ nanoparticles were modified with amine groups, immobilized with the structure of the
38 paper, and used to support the enzymes required for the selected tests. Therefore, the experiments
39 herein described address the criteria used for the selection of the conditions for the modification of the
40 nanoparticles, the adsorption of the enzyme, and the evaluation of the resulting analytical devices.
41
42
43
44
45
46
47
48
49

50 **3.1. Modification and deposition of the SiO₂ nanoparticles.** In order to enhance the protein adsorption
51 process and their immobilization to the cellulose, a silane-coupling reaction was carried out to introduce
52 amine groups on the surface of the silica nanoparticles. Although previously applied for the detection of
53 IgG using micro-zones plates, silica microbeads modified with this reaction have increased the adsorption
54
55
56
57
58
59
60

1
2
3 of proteins by 20-700%.⁴⁹ For this reaction, a solution of 5% (v/v) APTES was first prepared in ethanol.
4
5 Then, 3.3 mg of the SiO₂ nanoparticles were added to the solution and thoroughly mixed to form a
6
7 uniform suspension that was placed on an orbital shaker. Because a number of variables can affect the
8
9 density of amine groups^{50, 51} and the subsequent adsorption of the enzymes to the SiO₂ surface,⁵² the
10
11 effect of the time of contact between nanoparticles with APTES solution on the color intensity and color
12
13 gradient was first investigated. For these experiments, the SiO₂ nanoparticles were mixed with the
14
15 APTES solution and vortexed for different periods of time, ranging from 1 to 24 hours. Then, μ PADs were
16
17 immersed in the nanoparticle suspension, dried at room temperature and modified using the protocol for
18
19 glucose assay as described earlier. The results are summarized in Figure 1A. As it can be observed, the
20
21 modification time has significant effects on the color intensity but almost no effect on the color gradient
22
23 (within the experimental error). These results could be attributed to a balance between the amount of
24
25 protein adsorbed to the surface of the nanoparticles and the strength of the interaction. While at short
26
27 reaction times there may not be enough groups on the surface to support the enzyme dispensed, longer
28
29 reaction times could render the surface too hydrophobic; therefore inducing conformational changes in
30
31 the adsorbed enzyme and resulting in lower catalytic activities. Considering these results, particles
32
33 modified for 3 hours were used for the remaining experiments described in this manuscript.
34
35
36

37 These nanoparticles were deposited on the surface of the μ PAD via two different methods, either by
38
39 dispensing the suspension using an automatic pipette or by immersion. It was observed that when
40
41 particles (1 μ L of a suspension) were deposited on the surface of the μ PAD using a pipette, they
42
43 remained around the application point (data not shown). This behavior was attributed to the fact that even
44
45 small aggregates of the nanoparticles cannot move through the three-dimensional structure of the
46
47 cellulose and therefore tend to accumulate at the seeding point. In order to achieve a uniform distribution
48
49 of the nanoparticles, μ PADs were placed on a Petri dish, covered with a suspension of the nanoparticles,
50
51 and then left until the complete evaporation of the solvent (around 30 min). Before their use, the μ PADs
52
53 were rinsed with PBS to remove loosely-bound nanoparticles. Figure 1B shows a representative SEM
54
55 image of the detection zone after the modification with the SiO₂ nanoparticles. Considering that the most
56
57 homogenous distribution of nanoparticles would lead to a more homogeneous distribution of the enzymes
58
59
60

(and, consequently, better color uniformity), μ PADs prepared by immersion were used for the remaining experiments described in this manuscript.

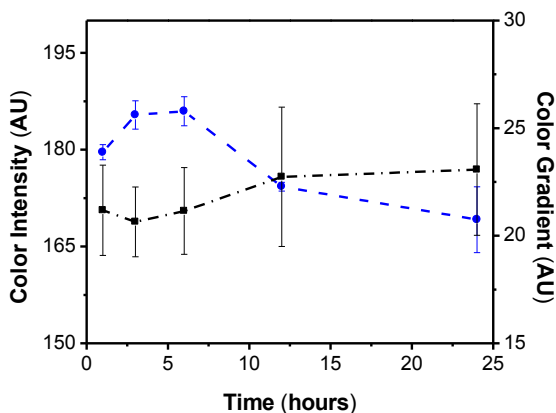


Figure 1A: Effect of modification time of silica nanoparticles with APTES on the color (●) intensity and (■) gradient.

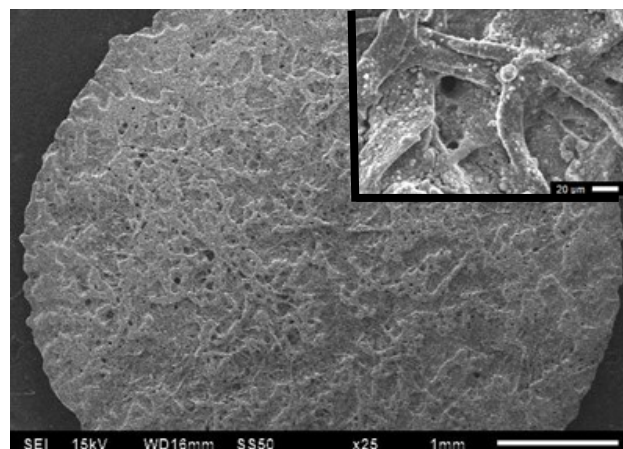


Figure 1B: SEM of the detection zone of a μ PAD after the deposition of SiO_2 nanoparticles by immersion.

3.2 Adsorption of GOx onto SiO_2 and $\text{SiO}_2/\text{APTES}$ Substrates. Being crystalline and highly charged, bare SiO_2 surfaces only allow for the adsorption of certain proteins.⁵³⁻⁵⁶ Therefore, and in order to increase the adsorption capacity of the surface, a modification with APTES was implemented. In order to determine the time required for the enzymes to saturate the surface and estimate the amount of protein immobilized, dynamic adsorption experiments were performed using GOx as the model enzyme. Although the curvature of the surface can also play a key role in the activity of the adsorbed protein,^{57, 58} the surface of the SiO_2 nanoparticle was mimicked using silica wafers, which were also modified using the procedure described for the nanoparticles. In order to prevent potential desorption of the enzyme upon the interaction with the urine sample, adsorption experiments were performed at pH = 6.0. Figure 2 shows a representative example of the dynamic adsorption experiments performed with GOx onto either the silica surface before (Si/SiO_2) or after the modification with APTES ($\text{Si}/\text{SiO}_2/\text{APTES}$).

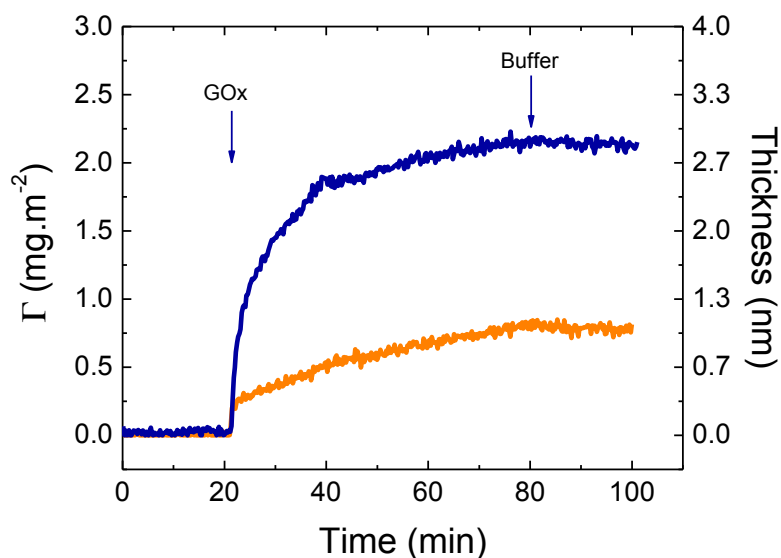


Figure 2: Adsorption of GOx ($1 \text{ mg}\cdot\text{mL}^{-1}$, $\text{pH} = 6.0$) onto either a Si/SiO_2 (orange curve) or a $\text{Si}/\text{SiO}_2/\text{APTES}$ (blue curve) substrate. The arrows show the time which the enzyme solution impinging on the substrate was replaced by the buffer solution.

As it can be observed for both cases, the adsorption proceeds as a fast process and gradually slows down as the surface coverage increased. It is important to note that while fast initial adsorption rates were obtained with both surfaces, significantly higher amounts were adsorbed upon the modification with APTES. For the case of the bare SiO_2 surfaces, the initial adsorption process ($d\Gamma/t_0 = 0.4 \pm 0.1 \text{ mg}\cdot\text{m}^{-2}\cdot\text{min}^{-1}$) quickly slowed down, leading to an adsorbed amount of only $0.8 \pm 0.1 \text{ mg}\cdot\text{m}^{-2}$ and a thickness of $1.1 \pm 0.1 \text{ nm}$ within the 80 min experiment. Considering the dimensions of the enzyme ($8.0 \text{ nm} \times 7.0 \text{ nm} \times 5.5 \text{ nm}^{59}$), these results suggest that a surface coverage of less than 20% was obtained within the timeframe investigated. For the case of $\text{Si}/\text{SiO}_2/\text{APTES}$, the adsorption of GOx also proceeded as a fast initial process ($d\Gamma/t_0 = 0.7 \pm 0.1 \text{ mg}\cdot\text{m}^{-2}\cdot\text{min}^{-1}$) and reached approximately 95% of the saturation amount within 20 min after the protein injection. Under these conditions, a GOx layer with a thickness of $2.7 \pm 0.1 \text{ nm}$ (corresponding to $\Gamma = 2.2 \pm 0.1 \text{ mg}\cdot\text{m}^{-2}$) was formed on the surface. These values suggest the formation of an incomplete monolayer on the surface, where GOx adopts a side-on conformation and a surface coverage of at least 50%. Experimental data also revealed that the protein layer could not be removed from the substrate when the buffer solution was allowed to impinge on the adsorbed protein film (Figure 2, at $t=80 \text{ min}$ for 20 min). This finding was considered fundamental as it demonstrated that the

1
2
3 enzyme remained on the surface (within the timeframe of the experiment) after a washing step, therefore
4
5 supporting the possibility to use adsorption as the immobilization method.
6
7

8
9 The difference in the behavior observed at both surfaces can be related to the nature of the
10 physicochemical interactions between the enzyme molecules and the solid surface. In general, the
11 adsorption process is driven by short- and long-range forces resulting from a combination of electrostatic
12 interactions between the protein and the solid surface,⁶⁰⁻⁶² co-adsorption of small ions, dispersion forces,
13 changes in the state of hydration of the sorbent surface and parts of the protein molecule, and structural
14 rearrangements in the protein.⁶³⁻⁶⁶ Consequently, the differences in thickness and adsorbed amount
15 observed between the Si/SiO₂ and Si/SiO₂/APTES substrates can be explained considering the role of
16 electrostatic interactions. At pH = 6 (the working pH), both the GOx (IEP = 4.2⁶⁷) and SiO₂ surface (IEP =
17 2.0⁶⁸) were negatively charged resulting in the adsorption process being limited by electrostatic repulsions
18 between the surface and the protein as well as between proteins. On the other side, when the surface
19 was modified with APTES (IEP = 7.4⁶⁹) the electrostatic interactions between the protein and the surface
20 were neutralized, resulting in a higher density of GOx on the surface. While these experiments were
21 performed with GOx, the similar structure of LOx and LGOx^{70, 71} suggests that a similar behavior can be
22 expected with the other enzymes.
23
24
25
26
27
28
29
30
31
32
33
34
35
36
37
38

39 **3.3 Analytical Performance.** In order to demonstrate the advantages of the proposed approach on the
40 analytical performance of μ PADs, the color intensity and uniformity of three enzymatic reactions was
41 evaluated. For this purpose, lactate, glucose, and glutamate were selected as target analytes. Since the
42 kidneys normally reabsorb them, no lactate or glucose are excreted into the urine when present in plasma
43 at normal levels. However, high levels of lactate (above 2.5 mM) can be found in patients with glycogen
44 storage disease type-I and may indicate that the liver may not be able to convert enough glucose from
45 glucose-6-phosphate.^{72, 73} As it is essential to manage and control diabetes⁷² and affects millions of
46 patients worldwide, glucose is one of the most assayed molecules. Elevated urinary glutamic acid levels
47 have been associated with a 4-fold higher risk for migraines in females.⁷⁴ Beyond their clinical relevance,
48 the three selected reactions are catalyzed by enzymes with well-known properties, and use a simple,
49
50
51
52
53
54
55
56
57
58
59
60

oxygen-dependent reaction that produces H_2O_2 .⁷⁵ The H_2O_2 is then utilized to oxidize a chromogenic agent in a secondary reaction catalyzed with HRP.⁷⁶

The enzymatic tests were performed on paper devices either with or without nanoparticles and prepared as described in the experimental section. As it can be observed in Figure 3, significant improvements in the signal intensity and color homogeneity were obtained when silica nanoparticles were used to support the enzymes. As previously hypothesized, the improvements in both intensity and uniformity can be explained by considering that silica nanoparticles, trapped within the three-dimensional structure of the cellulose, can provide a solid surface to immobilize the enzymes and therefore minimize the transport of the reactants as the solution wicks the device.

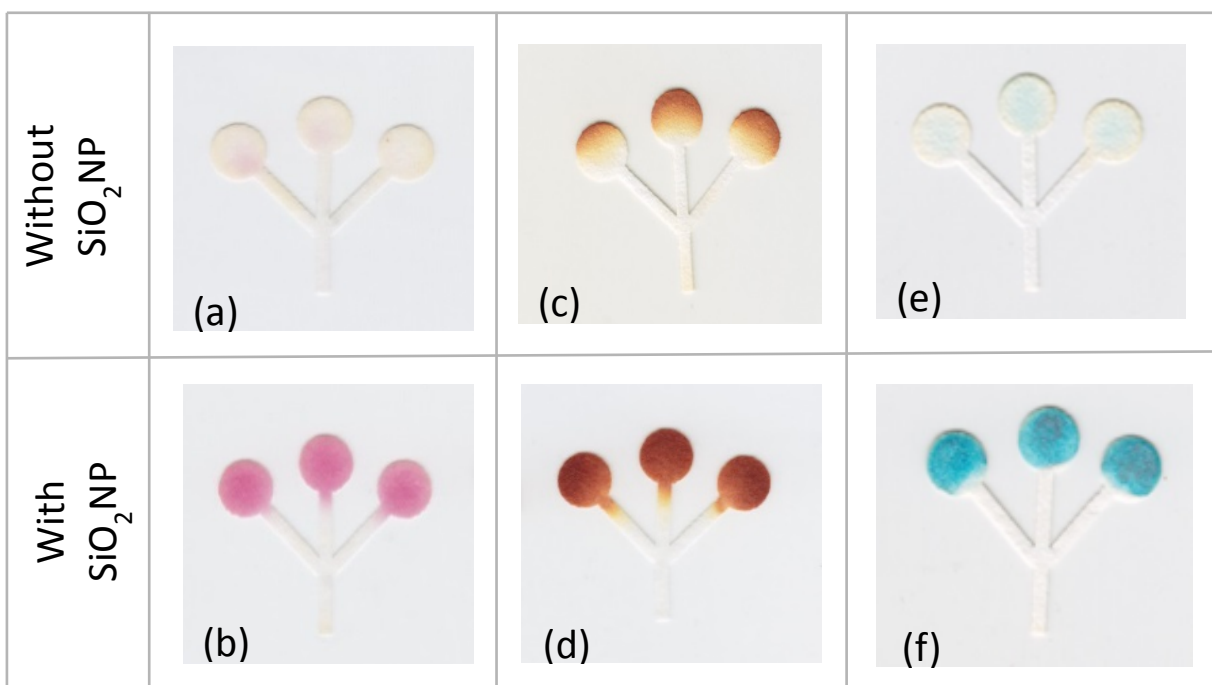


Figure 3: Optical images showing the colorimetric assays for (a, b) lactate, (c, d) glucose, and (e, f) glutamate assays on native (without SiO₂) and silica-modified (with SiO₂) papers. The concentrations for the lactate, glucose, and glutamate were 1.5, 20, and 10 mM, respectively.

Besides the visual evidence, the images were analyzed to obtain quantitative information of the effect of SiO₂ nanoparticles on the color intensity and homogeneity. It was observed (see *Supplementary Information*) that the addition of SiO₂ nanoparticles yielded improvements in color intensity (when compared with the same reaction on native paper) of 92%, 46% and 61% for the detection of lactate,

1
2
3 glucose, and glutamate tests, respectively. These values are related to the gain in color intensity taking
4 into account the values recorded on native paper by calculating the percent difference. Although the
5 addition of nanoparticles reduced the color gradient by 75% for the glucose assay, only slight
6 improvements were obtained for the lactate and glutamate assays. This difference can be attributed to
7 the poor color formed in the lactate and glutamate assays in the absence of the nanoparticles, therefore
8 skewing the results.
9
10
11
12
13
14
15
16

17 Calibration curves using nanoparticle-modified μ PADs were then generated by sequentially spotting the
18 reaction-zones with the reagents for lactate, glucose, and glutamate, and then mixtures of the
19 corresponding analytes at different concentration levels. Measurements were performed at least three
20 times and the mean intensity and relative standard deviations are shown in Figure 4. In general it can be
21 observed that within the investigated concentration range (0-10 mM), higher concentrations led to higher
22 color intensities. Under the optimized conditions also, linear relationships were obtained between the
23 concentration and the resulting color intensity for lactate (0.63 – 3.75 mM), glucose (0.5 – 10 mM), and
24 glutamate (0.25 – 7.50 mM). The limits of detection (LOD), calculated as the lowest concentration leading
25 to a signal that was proportional to the concentration of the analyte and with a magnitude of at least three
26 times the standard deviation of the blank, were 0.63 mM, 0.50 mM, and 0.25 mM for lactate, glucose, and
27 glutamate, respectively. In agreement with the trend shown in Figure 3, control calibration curves
28 performed for each analyte on devices fabricated without SiO_2 nanoparticles yielded to lower sensitivity
29 values and were significantly affected by signal heterogeneity (data not shown). It is also important to
30 highlight that while several batches of the μ PADs were used to collect the data reported in this
31 manuscript, no statistical difference was observed.
32
33
34
35
36
37
38
39
40
41
42
43
44
45
46
47
48
49
50
51
52
53
54
55
56
57
58
59
60

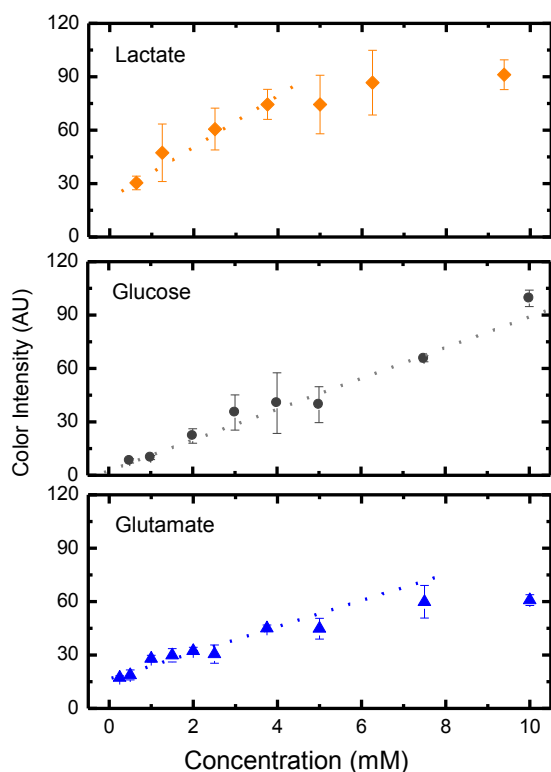


Figure 4: Calibration curves for lactate ($y=14x + 22$, $R^2=0.98$), glucose ($y=8.6x + 2$, $R^2=0.99$), and glutamate ($y=7.5x + 7$, $R^2=0.94$) assays performed on μ PADs containing chemically modified silica nanoparticles.

3.4 Analyses in Artificial Urine. The utility of the proposed μ PADs for the quantification of lactate, glucose, and glutamate levels in artificial urine samples was also investigated considering the clinically-relevant levels of lactate, glucose, and glutamate in urine.^{17, 38, 77} For these experiments, the artificial urine (prepared as described in the Experimental Section) was spiked with relevant concentrations of lactate (2.14 mM), glucose (7.33 mM), and glutamate (4.21 mM) and analyzed on μ PADs modified with SiO_2 nanoparticles. As it can be observed in Figure 5, the proposed μ PADs allowed the simultaneous analysis of the three analytes after the 30 min reaction. The color developed in each detection zone fell within the expected color intensity, calculated from each respective linear equation. Specifically, lactate was expected to have an intensity of 52 AU and the actual intensity was 58 ± 7 AU; glucose expected intensity was 66 AU and it read 71 ± 7 AU; and glutamate was expected to develop an intensity of 49 AU and read

1
2
3
4
5
6
7
8
9
10
11
12
13
14
15
16
17
18
19
20
21
22
23
24
25
26
27
28
29
30
31
32
33
34
35
36
37
38
39
40
41
42
43
44
45
46
47
48
49
50
51
52
53
54
55
56
57
58
59
60

57 ± 9 AU. These values (that are within one standard deviation of the expected results) were considered acceptable for the goals of the proposed project.

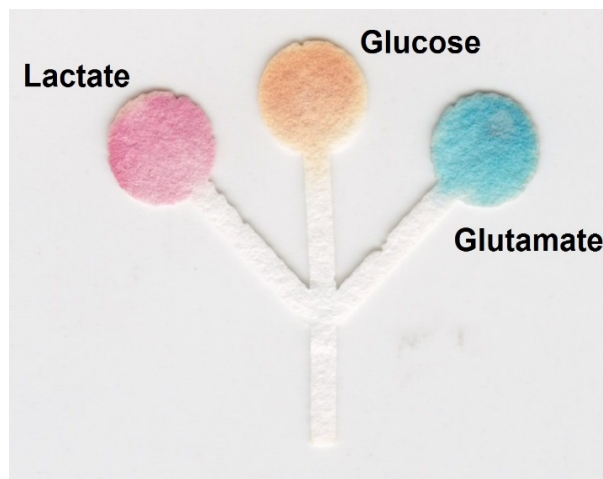


Figure 5: Optical image showing the analysis of an artificial urine sample spiked with lactate, glucose, and glutamate on the proposed μ PAD.

4. CONCLUSIONS

This current study has described a simple and rapid process to modify μ PADs with SiO₂ nanoparticles. The devices were fabricated using a CO₂ laser engraver and then immersed in a suspension containing the APTES-modified silica nanoparticles. These particles, trapped within the structure of the cellulose, served as a solid support to immobilize the enzymes responsible for the colorimetric reaction. By significantly improving the color intensity and color uniformity, the addition of these nanoparticles allows overcoming one of the major drawbacks of colorimetric detection on μ PADs. The platform was successfully applied to the qualitative (presence) and semi-quantitative analysis of lactate, glucose, and glutamate in urine samples. As such the devices can provide a strong platform to perform point-of-care testing in communities with limited resources. Furthermore, it is expected that other nanoparticles or nanomaterials will also allow the development of additional biochemical assays.

5. ACKNOWLEDGMENTS

Financial support for this project has been provided in part by the University of Texas at San Antonio, the National Institutes of Health through the Research Centers at Minority Institutions (G12MD007591), and the National Institutes of Health through the National Institute of General Medical Sciences

(2SC3GM081085). E.F.M.G gratefully acknowledges the scholarship granted from Conselho Nacional de Desenvolvimento Científico e Tecnológico (CNPq) and Instituto Nacional de Ciência e Tecnologia de Bioanalítica (INCTBio) – Science without borders program (Grant N^o 246903/2012-0).

6. REFERENCES

1. A. K. Yetisen, M. S. Akram and C. R. Lowe, *Lab Chip*, 2013, 13, 2210-2251.
2. X. Li, D. R. Ballerini and W. Shen, *Biomicrofluidics*, 2012, 6, 011301.
3. A. W. Martinez, S. T. Phillips, M. J. Butte and G. M. Whitesides, *Angewandte Chemie (International ed. in English)*, 2007, 46, 1318-1320.
4. W. Dungchai, O. Chailapakul and C. S. Henry, *Anal. Chim. Acta*, 2010, 674, 227-233.
5. W. K. Tomazelli Coltro, C.-M. Cheng, E. Carrilho and D. P. de Jesus, *Electrophoresis*, 2014, DOI: 10.1002/elps.201400006, n/a-n/a.
6. L. Ge, S. Wang, X. Song, S. Ge and J. Yu, *Lab Chip*, 2012, 12, 3150-3158.
7. Y. Sameenoi, P. Panyameesamer, N. Supalakorn, K. Koehler, O. Chailapakul, C. S. Henry and J. Volckens, *Environ. Sci. Technol.*, 2012, 47, 932-940.
8. D. M. Cate, W. Dungchai, J. C. Cunningham, J. Volckens and C. S. Henry, *Lab Chip*, 2013, 13, 2397-2404.
9. R. V. Taudte, A. Beavis, L. Wilson-Wilde, C. Roux, P. Doble and L. Blanes, *Lab Chip*, 2013, 13, 4164-4172.
10. A. W. Martinez, S. T. Phillips, G. M. Whitesides and E. Carrilho, *Anal. Chem.*, 2009, 82, 3-10.
11. Z. Nie, C. A. Nijhuis, J. Gong, X. Chen, A. Kumachev, A. W. Martinez, M. Narovlyansky and G. M. Whitesides, *Lab Chip*, 2010, 10, 477-483.
12. A. K. Ellerbee, S. T. Phillips, A. C. Siegel, K. A. Mirica, A. W. Martinez, P. Striehl, N. Jain, M. Prentiss and G. M. Whitesides, *Anal. Chem.*, 2009, 81, 8447-8452.
13. J. L. Delaney, C. F. Hogan, J. Tian and W. Shen, *Anal. Chem.*, 2011, 83, 1300-1306.
14. J. Yu, L. Ge, J. Huang, S. Wang and S. Ge, *Lab Chip*, 2011, 11, 1286-1291.
15. N. K. Thom, G. G. Lewis, M. J. DiTucci and S. T. Phillips, *RSC Adv.*, 2013, 3, 6888-6895.
16. J. Nie, Y. Liang, Y. Zhang, S. Le, D. Li and S. Zhang, *Analyst*, 2013, 138, 671-676.

- 1
2
3 17. W. Dungchai, O. Chailapakul and C. S. Henry, *Analytica Chimica Acta*, 2010, 674, 227-233.
4
5 18. S. A. Bhakta, R. Borba, M. Taba Jr, C. D. Garcia and E. Carrilho, *Anal. Chim. Acta*.
6
7 19. X. Chen, J. Chen, F. Wang, X. Xiang, M. Luo, X. Ji and Z. He, *Biosens. Bioelectron.*, 2012, 35,
8 363-368.
9
10 20. S. R. Mikkelsen and E. Corton, John Wiley & Sons, Inc., 2004, ch. 3, pp. 51-60.
11
12 21. S. A. Klasner, A. K. Price, K. W. Hoeman, R. S. Wilson, K. J. Bell and C. T. Culbertson, *Anal.*
13 *Bioanal. Chem.*, 2010, 397, 1821-1829.
14
15 22. M. Ornatska, E. Sharpe, D. Andreescu and S. Andreescu, *Anal. Chem.*, 2011, 83, 4273-4280.
16
17 23. F. Björkstén, *Biochim. Biophys. Acta*, 1970, 212, 396-406.
18
19 24. J. Hu, S. Wang, L. Wang, F. Li, B. Pingguan-Murphy, T. J. Lu and F. Xu, *Biosens. Bioelectron.*,
20 2014, 54, 585-597.
21
22 25. E. Evans, E. F. M. Gabriel, W. K. T. Coltro and C. D. Garcia, *Analyst*, 2014, 139, 2127-2132.
23
24 26. D. M. Lewis and K. A. McLlroy, *Rev. Prog. Color. Relat. Top.*, 1997, 27, 5-17.
25
26 27. D. Roy, M. Semsarilar, J. T. Guthrie and S. Perrier, *Chem. Soc. Rev.*, 2009, 38, 2046-2064.
27
28 28. K. Missoum, M. Belgacem and J. Bras, *Materials*, 2013, 6, 1745-1766.
29
30 29. G. Wegner, V. Buchholz, L. Ödberg and S. Stemme, *Adv. Mat.*, 1996, 8, 399-402.
31
32 30. J. Sirvio, U. Hyvakko, H. Liimatainen, J. Niinimaki and O. Hormi, *Carbohydr. Polym.*, 2011, 83,
33 1293-1297.
34
35 31. H. Koga, T. Kitaoka and A. Isogai, *J. Mat. Chem.*, 2011, 21, 9356-9361.
36
37 32. J. P. Lafleur, S. Senkbeil, T. G. Jensen and J. P. Kutter, *Lab Chip*, 2012, 12, 4651-4656.
38
39 33. W. W. Yu and I. M. White, 2011.
40
41 34. W. Dungchai, Y. Sameenoi, O. Chailapakul, J. Volckens and C. S. Henry, *Analyst*, 2013, 138,
42 6766-6773.
43
44 35. K. F. Lei, K.-F. Lee and S.-I. Yang, *Microelectron. Eng.*, 2012, 100, 1-5.
45
46 36. J.-W. Han, B. Kim, J. Li and M. Meyyappan, *RSC Adv.*, 2014, 4, 549-553.
47
48 37. A. W. Martinez, S. T. Phillips, E. Carrilho, S. W. Thomas, H. Sindi and G. M. Whitesides, *Anal.*
49 *Chem.*, 2008, 80, 3699-3707.
50
51
52
53
54
55
56
57
58
59
60

- 1
2
3 38. N. W. Tietz, *Clinical Guide to Laboratory Tests*, W.B. Saunders, Philadelphia, PA, 3rd edn.,
4 1995.
5
6
7 39. A. W. Martinez, S. T. Phillips, G. M. Whitesides and E. Carrilho, *Analytical Chemistry*, 2009, 82,
8 3-10.
9
10
11 40. A. K. Yetisen, M. S. Akram and C. R. Lowe, *Lab on a Chip*, 2013, 13, 2210-2251.
12
13 41. E. F. M. Gabriel, W. K. T. Coltro and C. D. Garcia, *Electrophoresis*, 2014, DOI:
14 10.1002/elps.201300511, n/a-n/a.
15
16
17 42. N. Z. Md Muslim, M. Ahmad, L. Y. Heng and B. Saad, *Sens. Actuators, B* 2012, 161, 493-497.
18
19 43. J. Yu, L. Ge, J. Huang, S. Wang and S. Ge, *Lab on a Chip*, 2011, 11, 1286-1291.
20
21 44. M. R. Nejadnik, L. Francis and C. D. Garcia, *Electroanalysis*, 2011, 23, 1462-1469.
22
23 45. M. F. Mora, M. Reza Nejadnik, J. L. Baylon-Cardiel, C. E. Giacomelli and C. D. Garcia, *J. Colloid*
24 *Interface Sci.*, 2010, 346, 208-215.
25
26
27 46. H. Fujiwara, *Spectroscopic ellipsometry. Principles and applications*, J. Wiley & Sons, West
28 Sussex, England, 2007.
29
30
31 47. M. R. Nejadnik, F. L. Deepak and C. D. Garcia, *Electroanalysis*, 2011, 23, 1462-1469.
32
33 48. Y. An, M. Chen, Q. Xue and W. Liu, *J. Colloid Interface Sci.*, 2007, 311, 507-513.
34
35 49. P. Bai, Y. Luo, Y. Li, X.-D. Yu and H.-Y. Chen, *Chin. J. Anal. Chem.*, 2013, 41, 20-24.
36
37 50. S. Ek, E. I. Iiskola, L. Niinistö, J. Vaittinen, T. T. Pakkanen, J. Keränen and A. Auroux, *Langmuir*,
38 2003, 19, 10601-10609.
39
40
41 51. J. R. Wayment and J. M. Harris, *Anal. Chem.*, 2006, 78, 7841-7849.
42
43 52. N. Aissaoui, L. Bergaoui, J. Landoulsi, J.-F. Lambert and S. Boujday, *Langmuir*, 2011, 28, 656-
44 665.
45
46
47 53. M. van der Veen, M. C. Stuart and W. Norde, *Colloids Surf. B*, 2007, 54, 136-142.
48
49 54. W. Norde, *Colloids Surf. B*, 2008, 61, 1-9.
50
51 55. E. N. Vasina, E. Paszek, D. V. N. Jr. and D. V. Nicolau, *Lab Chip*, 2009, 9, 891-900.
52
53 56. M. Rabe, D. Verdes and S. Seeger, *Adv. Colloid Interface Sci.*, 2011, 162, 87-106.
54
55 57. A. A. Vertegel, R. W. Siegel and J. S. Dordick, *Langmuir*, 2004, 20, 6800-6807.
56
57 58. M. Lundqvist, I. Sethson and B.-H. Jonsson, *Langmuir*, 2004, 20, 10639-10647.
58
59
60

- 1
2
3 59. H. J. Hecht, D. Schomburg, H. Kalisz and R. D. Schmid, *Biosens. Bioelectron.*, 1993, 8, 197-203.
4
5 60. Z.-H. Wang and G. Jin, *Colloids Surf. B*, 2004, 34, 173-177.
6
7 61. K. Yamada, S. Yoshii, S. Kumagai, I. Fujiwara, K. Nishio, M. Okuda, N. Matsukawa and I.
8 Yamashita, *Jpn. J. Appl. Phys.*, 2006, 45, 4259.
9
10 62. L.-S. Jang and H.-J. Liu, *Biomed. Microdevices*, 2009, 11, 331-338.
11
12 63. A. Baszким and W. Norde, eds., *Physical Chemistry of Biological Interfaces*, Marcel Dekker, Inc.,
13 New York, NY, 2000.
14
15 64. W. Norde and C. E. Giacomelli, *J. Biotechnol.*, 2000, 79, 259-268.
16
17 65. W. Norde, *Colloids Surf. B*, 2008, 61, 1-9.
18
19 66. A. W. P. Vermeer and W. Norde, *J. Colloid Interface Sci.*, 2000, 225, 394-397.
20
21 67. J. H. Pazur and K. Kleppe, *Biochemistry*, 1964, 3, 578-583.
22
23 68. M. Kosmulski, *J. Colloid Interface Sci.*, 1998, 208, 543-545.
24
25 69. H. Zhang, H.-X. He, J. Wang, T. Mu and Z.-F. Liu, *Appl. Phys. A* 1998, 66, S269-S271.
26
27 70. I. Zafar Hussain, S. Syed Muhammad Usman Ali, K. Kimleang and W. Magnus, *Sensors*, 2012,
28 12.
29
30 71. A. BÖHmer, A. MÜLLer, M. Passarge, P. Liebs, H. Honeck and H.-G. MÜLLer, *Eur. J. Biochem.* ,
31 1989, 182, 327-332.
32
33 72. C.-C. Lin, C.-C. Tseng, T.-K. Chuang, D.-S. Lee and G.-B. Lee, *Analyst*, 2011, 136, 2669-2688.
34
35 73. T. Hagen, M. S. Korson and J. I. Wolfsdorf, *Mol. Gen. Metab.*, 2000, 70, 189-195.
36
37 74. C. Ragginer, A. Lechner, C. Bernecker, R. Horejsi, R. Möller, M. Wallner-Blazek, S. Weiss, F.
38 Fazekas, R. Schmidt, M. Truschnig-Wilders and H. J. Gruber, *Eur. J. Neurol.*, 2012, 19, 1146-
39 1150.
40
41 75. A. Alnokkari, M. Ataie and Z. Alasaf, *Chin. J. Appl. Environ. Biol.*, 2013, 19, 1069-1072.
42
43 76. X. Chen, J. Chen, F. Wang, X. Xiang, M. Luo, X. Ji and Z. He, *Biosensors and Bioelectronics*,
44 2012, 35, 363-368.
45
46 77. A. H. B. Wu, *Tietz clinical guide to laboratory tests*, Saunders/Elsevier, St. Louis, Mo., 4th edn.,
47 2006.
48
49
50
51
52
53
54
55
56
57
58
59
60